Amorphous calcium carbonate transforms into calcite during sea urchin larval spicule growth

ELIA BENIASH, JOANNA AIZENBERG, LIA ADDADI AND STEPHEN WEINER

Department of Structural Biology, Weizmann Institute of Science, 76100 Rehovot, Israel

SUMMARY

Sea urchin larvae form an endoskeleton composed of a pair of spicules. For more than a century it has been stated that each spicule comprises a single crystal of the $CaCO_3$ mineral, calcite. We show that an additional mineral phase, amorphous calcium carbonate, is present in the sea urchin larval spicule, and that this inherently unstable mineral transforms into calcite with time. This observation significantly changes our concepts of mineral formation in this well-studied organism.

1. INTRODUCTION

The sea urchin embryo has been a favourite subject of research in developmental biology for over a century (Theel 1892; Livingston & Wilt 1990; Cameron & Davidson 1991; Davidson 1993). Larval spicule formation has also been studied extensively (Decker & Lennarz 1988; Wolpert & Gustafson 1961; Wilt & Benson 1988; Ettensohn & Malinda 1993; Armstrong & McClay 1994). The larvae form an elaborate endoskeleton composed of two spicules, each one of which is a single crystal of magnesium-bearing calcite (Wilt & Benson 1988). Spiculogenesis takes place in a membrane-delineated compartment, inside a syncytium formed by specialized mesodermal cells. It has been observed that the initial mineral deposit of each spicule is a rhombohedral-shaped crystal typical of calcite (Theel 1892; Okazaki & Inoue 1976) that forms in the early gastrula stage. Further growth is in the form of smooth rounded rods that grow along the *a*-axes of the initial crystal (Wolpert & Gustafson 1961; Okazaki & Inoue 1976). The triradiate spicules form within about 5 h. During the next stage of spiculogenesis two of the radii change their growth direction by 90°, forming so called rods growing along the *c*-axis of calcite. The spicules are fully formed when the larvae reach the pluteus stage (figure 1). If the larvae are not fed, spicule development ceases, even though the larvae can continue to live for several more days.

The process of sea urchin larval endoskeleton formation appears thus to be ideally suited for the study of mechanisms involved in mineral transport, deposition and transformation. Its development can be followed within an easily manageable time range, the crystal size is large enough to allow characterization by X-rays and the first deposits in and around the spicular cavity can be studied by electron microscopy. In this context in particular, electron-dense, calcium-rich granules have been observed in the cytoplasm of spiculogenic cells (Decker *et al.* 1987). It was consequently suggested that components of the spicules, especially the mineral and possibly associated glycoproteins, may be preassembled intracellularly and delivered to the spicular cavity through vesicular transport.

Here we show that amorphous $CaCO_3$ is present during the first stages of spicule growth in large amounts, relative to the total mineral deposit, and that this transforms with time into calcite. This observation is important for the understanding of mineral formation in the sea urchin larva. It constitutes also the first documentation of amorphous $CaCO_3$ transforming into calcite in biology, an event that may well be more widespread, but is extremely difficult to observe.

2. MATERIALS AND METHODS

The larvae of *Paracentrotus lividus* were cultured using standard methods in Millipore filtered seawater at 18 °C without feeding (Giudice 1973). To obtain clean spicules, the suspensions of larvae in 50 ml plastic tubes were centrifuged for 2–5 min at 1000 rpm. The supernatant was replaced with saturated glucose solution and the samples were centrifuged again. The pellet was resuspended in an equal volume of glucose solution and transferred into cooled Eppendorf 1.5 ml tubes (0.5 ml per tube). Each tube was shaken for 10 s and 1 ml of 4 % NaOCl solution was added. The tube was shaken for an additional 20 s and briefly (2–5 s) centrifuged. The supernatant was substituted with 2.5 % NaOCl. After 20 min at room temperature, the spicules were briefly (few seconds) rinsed three times in double-distilled water and dried under vacuum. For scanning electron microscopy, spicules were dried on aluminum stubs, gold-coated and observed under a JEOL 6400 scanning electron microscope (SEM).

X-ray measurements were performed on a Rigaku rotating Cu-anode four-circle diffractometer. The diffraction peak profiles were collected in the ω-scan mode for selected individual spicules of identical shapes and sizes. Three symmetry-related {104} reflections were monitored for three

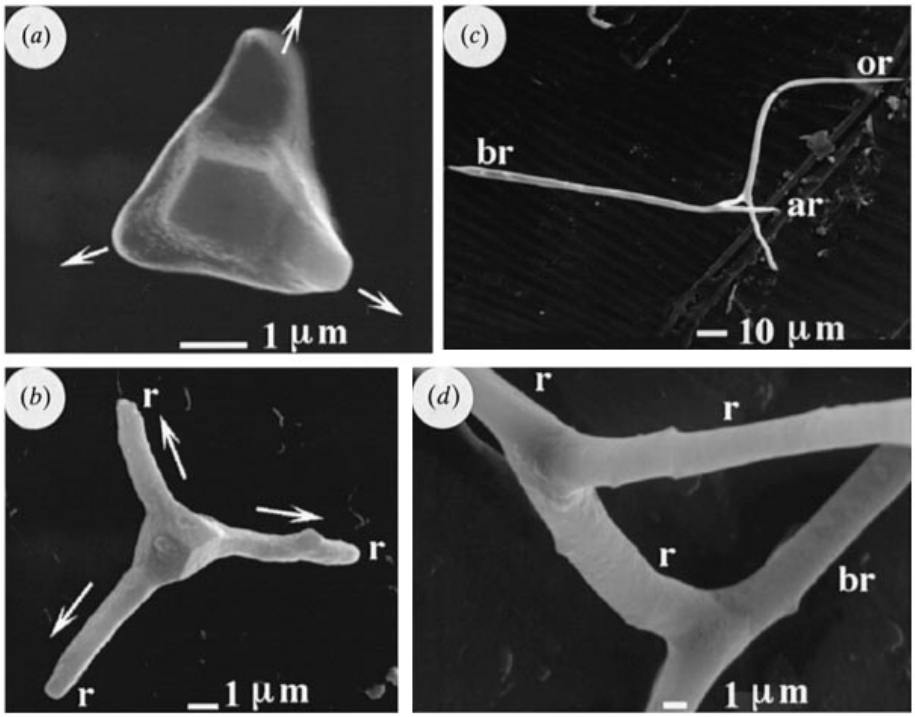

Figure 1. Sea urchin, *Paracentrotus lividus*, larval spicules at different developmental stages. (*a*) The earliest stage of spiculogenesis (20 h embryo) showing a rhombohedral-shaped crystal typical of calcite, and three radii starting to grow from this crystal (*a*-axes directions are indicated by arrows). (*b*) Triradiate spicule (25 h embryo) composed of the initial crystal and three radii growing along the *a*-axes (indicated by arrows). (*c*) Fully developed pluteus spicule (48 h embryo) composed of the central triradiate portion and three rods growing roughly in the *c*-axis direction. (*d*) Central triradiate portion of the pluteus spicule (48 h embryo) showing that the faceted calcite crystal is now not visible. r, radii; br, body rod; ar, anal rod; or, oral rod.

spicules of each age group. Each profile consisted of 40 data points with sampling frequencies of 0.02°. The control synthetic calcite crystal was measured under the same conditions. The volumes of the spicules and the volume of the measured calcite crystal were then calculated from SEM micrographs.

For infrared spectroscopy the dried and ground samples were mounted in KBr pellets. Infrared absorption spectra were obtained using a MIDAC Fourier transform infrared (FTIR) spectrometer.

For the etching experiments the clean spicules were immersed in double distilled water and 1 M KOH for 10 h with gentle rocking. After the treatment the spicules were briefly washed with double-distilled water, dried on aluminum stubs, gold-coated and observed under a JEOL 6400 scanning electron microscope.

3. RESULTS

The first hint that an amorphous phase may be present in the larval spicule was that the intensities of X-ray reflections obtained from a single pluteus spicule were much lower than those obtained from a calcite crystal of the same volume (Berman *et al*. 1993). We then measured the X-ray diffraction intensities of the {104} family of reflections of pluteus spicules of the sea urchin, *P. lividus*, 48 h and 96 h after fertilization (figure 2). The larvae of *P. lividus* grown in the culture without feeding reach the pluteus stage and then development ceases after 48 h. We cultured them for an additional 48 h and no changes in morphology were noted. Both the 48 h and 96 h groups of spicules were similar in size and morphology, and fractured surfaces did not reveal the presence of any internal

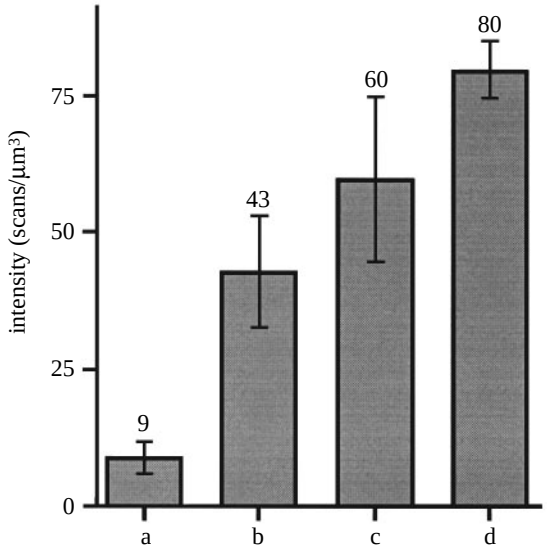

Figure 2. Average integrated intensities of {104} reflections of individual spicules obtained by X-ray diffraction: (a) 48 h, (b) 96 h pluteus spicules, (c) 96 h pluteus spicules stored dried in a freezer for four months, (d) synthetic calcite crystal. The intensities were normalized to a volume of 1 μm^3; bars indicate ± standard deviation.

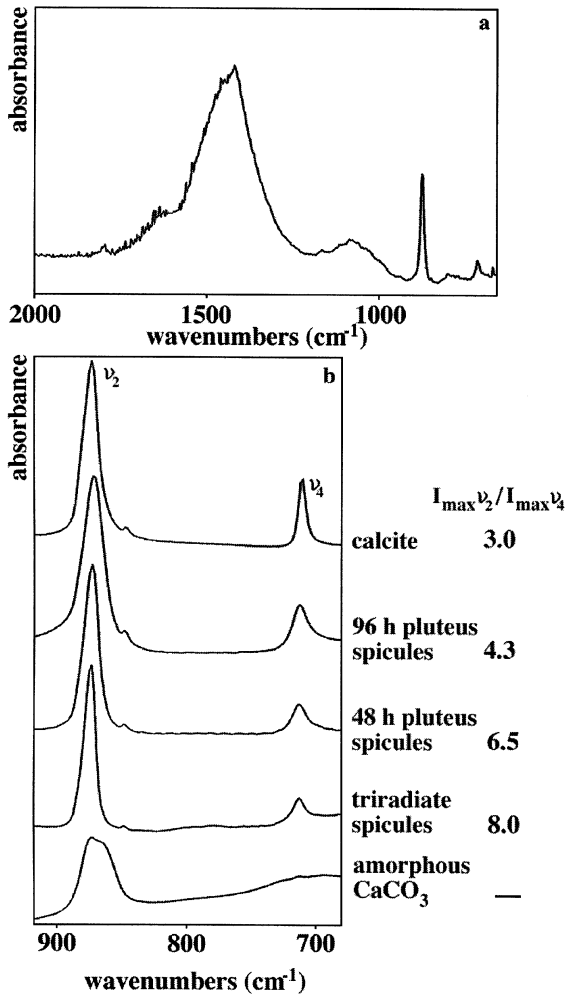

Figure 3. (*a*) Infrared spectrum of sea urchin larval spicules. The peak at 1420 cm^{-1} corresponds to the ν_3 absorption band; the broad peak centred at 1086 cm^{-1} belongs to the ν_1 absorption band of amorphous $CaCO_3$; the peaks at 874 and 713 cm^{-1} correspond to ν_2 and ν_4 absorption bands of calcite, respectively. (*b*) Portions of the infrared spectra of amorphous $CaCO_3$, three spectra of sea urchin larval spicules at different stages of development and geological calcite, showing the ν_2 and ν_4 absorptions. The ratios of the maximal intensities of the ν_2 versus the ν_4 absorption bands are presented.

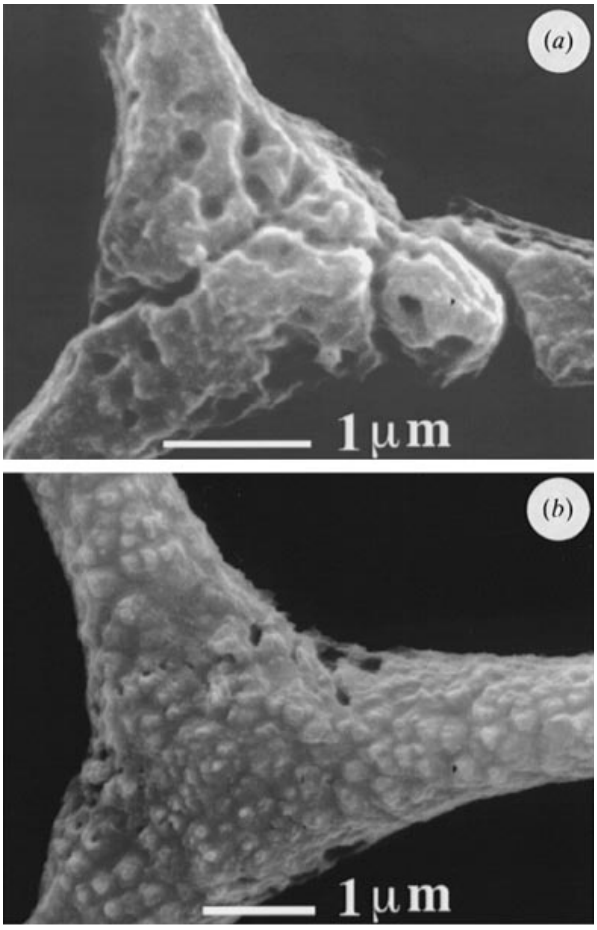

Figure 4. SEM micrographs of the surfaces of triradiate sea urchin spicules after etching with (*a*) double-distilled water and (*b*) 1N KOH.

cavities. The X-ray diffraction intensities per unit volume of the larval spicules are much lower than those of the synthetic calcite crystal. This implies that additional mineral is present, over and above the single crystal of calcite. Furthermore, the diffraction intensities of the 96 h larval spicules are about five times greater than those of the 48 h larval spicules, indicating that more calcite is present in the former even though the spicules in both groups are morphologically the same and similar in volume (figure 2).

The mineral phase present is calcite-based on the ν_4 and ν_2 absorption bands of $CO_3^=$ ions at 713 cm^{-1} and 874 cm^{-1}, respectively (figure 3*a*) (Chester & Elderfield 1967). The presence of a broad ν_1 band around 1086 cm^{-1} which is not infrared active in calcite (figure 3*a*) is consistent with the presence of amorphous $CaCO_3$ in the spicules(Brecevic & Nielsen 1989; Aizenberg *et al*. 1996), although organic material could also contribute to this broad absorption. The fact that amorphous $CaCO_3$ does not have a ν_4 absorption band in the 713 cm^{-1} region and has a broad ν_2 absorption pattern around 866 cm^{-1} (figure 3*b*) (Aizenberg *et al*. 1996) implies that if the spicule is mainly a mixture of calcite and amorphous calcium carbonate, the ratios of the maximal intensities of the ν_2 and ν_4 absorption peaks should be higher than those of calcite. This was indeed observed for larval spicules of different ages (figure 3*b*). It is very difficult to estimate even semi-quantitatively the proportions of the two mineral phases, as the absorption coefficient of the amorphous phase ν_2 peak at 866 cm^{-1} is much less than that of calcite at 875 cm^{-1}, and the former peak is also much broader than the calcite peak. The observed trends in figure 3 could, alternatively, be due to the presence of intermediate transformation phases between the amorphous and crystalline end members. Infrared spectra of biogenic amorphous calcium carbonate (from *Pyura pachydermatina*) (Lowenstam 1989) transformed into calcite by gentle heating, and obtained under the same conditions as those in figure 3, showed a decrease in the width at half height of the ν_4 absorption pattern with increasing extent of transformation. In contrast, the widths at half height of the same peak from the larval spicules remained constant with increasing age (figure 3*b*). The observed trend in figure 3*b* is therefore consistent with the proportions of calcite increasing with increasing age of the larvae.

The larval spicules can be etched readily by distilled water and 1 M KOH (figure 4). Under the conditions used neither of these treatments affects pure calcite. It is of interest to note that the ratio of the maximal intensities of ν_2 and ν_4 absorption peaks in the infrared spectra of the late triradiate spicules etched with distilled water is significantly less than the untreated spicules of the same age (5.5 versus 8.0 respectively). This is also consistent with the presence of an amorphous $CaCO_3$ phase having been removed, or having recrystallized into calcite during treatment.

All the above observations show that sea urchin larval spicules are composed of two mineral phases: calcite and amorphous $CaCO_3$. Furthermore, the proportions of the amorphous phase decrease in favour of calcite with increasing age of the larvae.

4. DISCUSSION

Amorphous $CaCO_3$ is a metastable phase that may form in supersaturated solutions of calcium and carbonate, but transforms within minutes into the stable crystalline phase (Brecevic & Nielsen 1989; Clarkson *et al*. 1992). Some organisms are able to form stable amorphous $CaCO_3$ (Lowenstam & Weiner 1989). Most biogenic deposits of amorphous $CaCO_3$ are used as temporary storage sites for calcium and carbonate. Perhaps the most common occurrence is in plants. These cystoliths readily transform into calcite *in vitro* but not *in vivo* (Taylor *et al*. 1993). In certain ascidian and sponge spicules amorphous calcium carbonate is, however, used as a structural material, and it has been shown *in vitro* for both that specific proteins are responsible for the stabilization of the amorphous phase (Aizenberg *et al*. 1996). The sponge spicules also contain a separate layer of calcite, but there is no evidence that the amorphous phase transforms into calcite (Aizenberg *et al*. 1996). The sea urchin larval spicule is thus the first example in biology of amorphous $CaCO_3$ acting as a transient precursor of the more stable mineral phase, the single crystal of calcite. As the presence of the amorphous phase together with calcite is easily overlooked, we suspect that this phenomenon may be more widespread.

Eight examples in biology of precursor minerals transforming into different mature minerals are listed by Lowenstam & Weiner (1989). One case, the marine cyanobacterium genus, *Rivularia*, is purported to involve the transformation of amorphous calcium carbonate to aragonite, based only on morphological evidence (Golubic & Campbell 1980). All the others involve iron oxide minerals, vaterite to aragonite transformation, or amorphous calcium phosphate transforming into a variety of crystalline phases. In one relatively well documented case, the teeth of certain molluscs (Chitonidae), amorphous calcium phosphate is stabilized for some two weeks, and then begins transforming to dahllite within a 24 h period (Lowenstam & Weiner 1985).

Amorphous phases in biology can thus be stabilized permanently, or for relatively long periods of time and then transform rapidly into the crystalline phase (Lowenstam & Weiner 1985; Aizenberg *et al*. 1996). In the case of the sea urchin larva, an initial crystalline mineral phase is formed, followed by an amorphous phase, which being unstable, transforms into calcite. The fact that the initial mineral deposit is a calcite crystal oriented in a very specific manner with respect to the syncytium (Wolpert & Gustafson 1961) implies that the nucleation of this crystal must be very well controlled. The growth of the three arms of the triradiate stage spicule is clearly influenced by the initial crystal orientation as they extend in the directions of the *a*-axes (figure 1*b*). We can only surmise that this proceeds by the deposition of the amorphous phase followed by its gradual transformation into the crystalline phase. This transformation must be to a large extent mediated by cells. The transformation in the spicule is much slower than that of pure amorphous calcium carbonate (Brecevic & Nielsen 1989; Clarkson *et al*. 1992). It is also much faster than the transformation which occurs in dried spicules removed from the larvae (figure 2*c*). The presence of the amorphous phase may reflect the fact that the mineral is delivered into the spicular cavity in this form through vesicles, as suggested by the presence of electron-dense calcium-rich granules in spicule-forming cells (Decker *et al*. 1987). Alternatively, the amorphous phase may form directly due to very high concentrations of calcium and carbonate in the mineralization compartment.

At this stage we can only speculate about the mechanism of transformation. As no new calcite crystals form during growth of the spicule, we deduce that the increase in calcite content is only due to the growth of the initial single crystal. This most probably occurs by local dissolution of the amorphous phase and reprecipitation on the crystal surface. It is even more difficult to understand the benefits that this mode of growth affords to sea urchin larvae. One possibility is that this is a means of rapidly forming the skeleton. Indeed spicules elongate at their tips at the rate of about $5\,\mu m\,h^{-1}$: a remarkably rapid rate. The amorphous precursor phase may also facilitate the process of shaping of the spicules, or possibly even help the organism to stay buoyant by the use of material that is less dense than calcite.

The observation that larval spicule formation involves two mineral phases significantly adds to our understanding of spiculogenesis. It therefore needs to be integrated into the many detailed studies of the genetic, molecular and cellular control mechanisms of sea urchin larval spicule formation. The implications may extend to the process of skeleton formation in adult echinoderms, and possibly to other phyla as well.

We thank Dr Fred Wilt, University of California, Berkeley, for advising us about sea urchin larval culture and spicule preparation techniques. S.W. is the incumbent of the I. W. Abel Professorial Chair of Structural Biology, and L.A. of the Patrick E. Gorman Professorial Chair of Biological Ultrastructure. This study was funded in part by the Kimmelman Center for Biomolecular Structure and Assembly and by grant No. 92–00100 from the US–Israel Binational Science Foundation.

REFERENCES

Aizenberg, J., Lambert, G., Addadi, L. & Weiner, S. 1996 Stabilization of amorphous calcium carbonate by specialized macromolecules in biological and synthetic precipitates. *Adv. Mater.* **8**, 222–226.

Armstrong, N. & McClay, D. R. 1994 Skeletal pattern is specified autonomously by the primary mesenchyme cells in sea urchin embryos. *Dev. Biol.* **162**, 329–338.

Berman, A., Hanson, J., Leiserowitz, L., Koetzle, T. F., Weiner, S. & Addadi, L. 1993 Biological control of crystal texture: a widespread strategy for adapting crystal properties to function. *Science, Wash.* **259**, 776–779.

Brečević, L. & Nielsen, A. 1989 Solubility of amorphous calcium carbonate. *J. Crystal Growth* **98**, 504–510.

Cameron, R. A. & Davidson, E. H. 1991 Cell type specification during sea urchin development. *Trends Genet.* **7**, 212–218.

Chester, R. & Elderfield, H. 1967 The application of infra-red absorption spectroscopy to carbonate mineralogy. *Sedimentology* **9**, 5–21.

Clarkson, J. R., Price, T. J. & Adams, C. J. 1992 Role of metastable phases in the spontaneous precipitation of calcium carbonate. *J. Chem. Soc. Faraday Trans.* **88**, 243–249.

Davidson, E. H. 1993 Later embryogenesis: regulatory circuitry in morphogenetic fields. *Development* **118**, 665–690.

Decker, G. L. & Lennarz, W. J. 1988 Skeletogenesis in the sea urchin embryo. *Development* **103**, 231–247.

Decker, G. L., Morrill, J. B. & Lennarz, W. J. 1987 Characterization of sea urchin primary mesenchyme cells and spicules during biomineralization *in vitro*. *Development* **101**, 297–312.

Ettensohn, C. A. & Malinda, K. M. 1993 Size regulation and morphogenesis—a cellular analysis of skeletogenesis in the sea urchin embryo. *Development* **119**, 155–167.

Giudice, G. 1973 *Developmental biology of the sea urchin embryo*. New York and London: Academic Press.

Golubic, S. & Campbell, S. E. 1980 Biologically-formed aragonite concretions in marine *Rivularia*. In *Phanerozoic stromatolites*. New York: Springer-Verlag, pp. 209–229.

Livingston, B. T. & Wilt, F. H. 1990 Determination of cell fate in sea urchin embryos. *Bioessays* **12**, 115–119.

Lowenstam, H. A. 1989 Spicular morphology and mineralogy of some Pyuridae (Ascidiacea). *Bull. Mar. Sci.* **45**, 243–252.

Lowenstam, H. A. & Weiner, S. 1985 Transformation of amorphous calcium phosphate to crystalline dahllite in the radular teeth of chitons. *Science, Wash.* **227**, 51–53.

Lowenstam, H. A. & Weiner, S. 1989 *On biomineralization*. Oxford University Press.

Okazaki, K. & Inoue, S. 1976 Crystal property of the larval sea urchin spicule. *Dev. Growth Differ.* **18**, 413–434.

Taylor, M. G., Simkiss, K., Greaves, G. N., Okazaki, M. & Mann, S. 1993 An X-ray-absorption spectroscopy study of the structure and transformation of amorphous calcium-carbonate from plant cystoliths. *Proc. R. Soc. Lond.* B **252**, 75–80.

Theel, H. 1892 On the development of *Ehinocyamus pusillus*. *Nova Acta Res. Soc. Sci. Upsala* **15**, 1–57.

Wilt, F. & Benson, S. 1988 Development of the endoskeletal spicule of the sea urchin embryo. In *Self-assembling architecture*. New York: Alan R. Liss, Inc., pp. 203–227.

Wolpert, L. & Gustafson, T. 1961 Studies of the cellular basis of morphogenesis of the sea urchin embryo (Development of the skeletal pattern). *Exp. Cell Res.* **25**, 311–325.

Received 7 October 1996; accepted 5 November 1996